Rotor Design Options for Improving Tiltrotor Whirl-Flutter Stability Margins



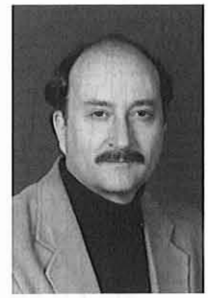

C. W. Acree, Jr.
NASA Ames Research Center

R. J. Peyran
U.S. Army Aeroflightdynamics Directorate

Wayne Johnson
NASA Ames Research Center

Rotor design changes intended to improve tiltrotor whirl-flutter stability margins were analyzed. A baseline analytical model similar to the XV-15 (23% thick wing) was established, and then a 15% thick wing was designed to be representative of a high-speed tiltrotor. While the thinner wing has lower drag, it also has lower stiffness, reducing whirl-flutter stability. The rotor blade design was modified to increase the stability speed margin for the thin-wing design. Small rearward offsets of the aerodynamic-center locus with respect to the blade elastic axis created large increases in the stability boundary. The effect was strongest for offsets at the outboard part of the blade, where an offset of the aerodynamic center by 10% of tip chord improved the stability margin by over 100 knots. Forward offsets of the blade center of gravity had similar but less pronounced effects. Equivalent results were seen for swept-tip blades. Combinations of tip sweep, control-system stiffness, and delta-three were also investigated. A limited investigation of blade loads in helicopter and airplane configuration indicated that proper choice of parametric variations can avoid excessive increases in rotor loads.

Notation

AC	blade section aerodynamic center, positive aft of EA
CG	blade chordwise center of gravity, positive forward of EA
C_T/σ	thrust coefficient, divided by solidity
EA	elastic axis
QC	blade quarter chord, positive aft of EA
R	rotor radius
t/c	wing thickness-to-chord ratio
Δ	change in blade chordwise QC or CG position
δ_3	kinematic pitch-flap coupling ratio
μ	advance ratio (flight speed divided by tip speed)

Introduction

Coupled wing/rotor whirl-mode aeroelastic instability is the major barrier to increasing tiltrotor speeds. Increased power, thrust, and rotor efficiency are of no avail unless the whirl-mode stability boundary can be improved. With current technology, very stiff, thick wings of limited aspect ratio are essential to meet the stability requirements, which severely limits cruise efficiency and maximum speed. Reference 1 gives a brief history of tiltrotor aeroelastic stability research and its application to tiltrotor design and flight test.

Numerous approaches to improving the whirl-mode airspeed boundary have been investigated, including tailored stiffness wings (Refs. 2–5), active stability augmentation (Ref. 6), variable geometry rotors (Ref. 7), highly swept tips (Ref. 8), and at one extreme, folding rotors (Ref. 9). The research reported herein took an alternative approach of adjusting the chordwise positions of the rotor blade aerodynamic center and center of gravity, effected by offsetting the airfoil quarter chord or structural mass with respect to the elastic axis. The results implied the desirability of swept blades, hence the research was extended to include variations in blade sweep. The effects of control system stiffness and delta-three on stability were also studied in conjunction with sweep. The consequences for blade loads were briefly assessed. The XV-15 rotor was the baseline.

Srinivas, Chopra, and Nixon (Ref. 8) also examined the effects of blade sweep on whirl flutter for a rotor similar to the XV-15. The present research was conducted independently of that reported in Ref. 8, and used a different analytical method. Reference 8 studied the effects of tip anhedral (droop) and taper, but not control stiffness or delta-three. Other differences are discussed in context, below.

Analytical Model

A CAMRAD II model of a notional tiltrotor was developed to serve as a baseline for parametric variations of rotor design parameters. The new model was based closely on an existing model of the XV-15, chosen because it is well-proven for stability analysis and thoroughly understood by the authors. See Refs. 10 and 11 for correlation of CAMRAD predictions with measured stability and loads.

Figure 1 illustrates the XV-15 with pertinent dimensional data; the moderate aspect ratio of the thick wing is clearly evident. (Detailed specifications are given in Ref. 12; see also Ref. 1.) The model used here was altered in several ways from the actual XV-15, including a different wing, a simplified drive train, and deletion of wing aerodynamic damping. The changes are discussed further below.

Airframe

Considerable effort was put into creating a thin, high-speed wing design that could be rigorously compared to the actual XV-15 wing. The new wing has the same planform as the XV-15 wing, but with a thickness-to-chord ratio (t/c) of 15%, a value typical of current commuter aircraft, instead of 23%. Airframe drag was arbitrarily reduced by 25% to simulate

Manuscript received January 2000; accepted January 2001.

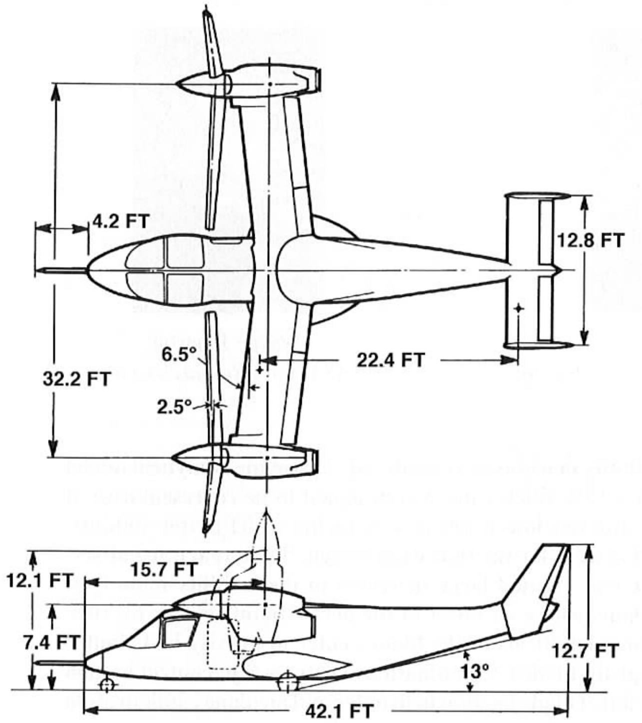

Fig. 1. XV-15 tiltrotor aircraft geometry, with 23% t/c wing (Ref. 12).

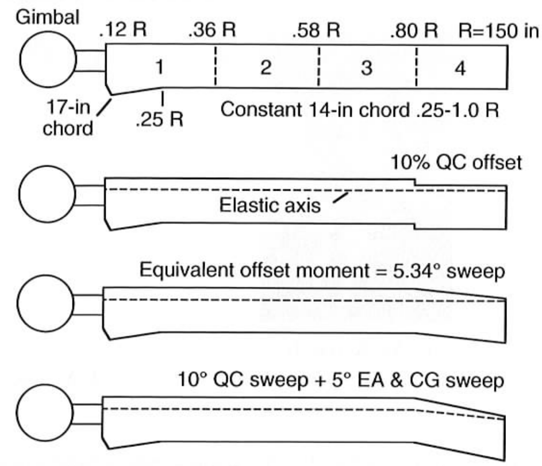

Fig. 2. XV-15 rotor blade planform (45-deg twist and 1-deg baseline sweep not shown).

the improved aerodynamics expected from a thinner wing and other drag improvements typical of a high-speed design. The new wing was designed strictly for strength; no allowance was made for aeroelastic stability.

To calculate aeroelastic stability, CAMRAD II couples externally generated wing modes to internally generated rotor modes (Ref. 13). Merely lowering the wing frequencies does not result in mode shapes realistic for a thinner wing. The new wing was modeled in NASTRAN (Ref. 14) to get modal data for input into CAMRAD II. The design and validation of the new wing model are documented in Ref. 15.

The XV-15 airframe model evolved through three stages. Details are given in Ref. 15; a brief summary is given here. The original CAMRAD II model utilized wing mode shapes and frequencies generated by a detailed NASTRAN model. The second model used NASTRAN data from a much simpler "stick" model of the original, 23% t/c wing; this is denoted the "thick wing" model. The third model, used in this study as a baseline reference, used NASTRAN data from a stick model of a 15% t/c wing; this is denoted the "thin wing" model. The two NASTRAN stick models differed only in the parameters affected by wing thickness, thereby ensuring that comparisons between the thick and thin wings were not affected by differences in NASTRAN modeling methods.

The primary purpose of the thinner wing, at least as it applies to the present research, is to lower the whirl-mode airspeed stability boundary to better reveal the effects of parametric variations of the rotor. Because the rotor was not redesigned for higher speeds, the thin wing is of limited value for increasing cruise performance. Nevertheless, the new wing provides an adequate baseline, so the notional model was not further optimized.

Rotor

The baseline rotor used in the study was the original XV-15 steel-blade rotor, with a 2.5-deg precone titanium hub and −15-deg delta-three (nominal). This is a rigid (stiff-in-plane) rotor with a gimbaled hub (Ref. 12). The inboard aerodynamic sections start with a 17-in chord at 12% radius, linearly tapering to a 14-in chord at 25% radius; the chord is constant from there to the tip (Fig. 2). Total effective blade twist is 45 deg over a 150-in radius. The entire blade has a 1-deg aft aerodynamic sweep, with the quarter-chord line intersecting the pitch axis at 75% radius.

For all cases analyzed, the rotor was modeled in CAMRAD II (Ref. 13) with a gimbal, two bending modes, one torsion mode, and flexible pitch links. The left-right symmetry of the XV-15 was exploited by calculating symmetric and antisymmetric modes separately. A "rigid" drive train model included the engine and gearbox inertias, but not drive-train flexibility or damping. (A full drive-train model would be needed for analysis of a production rotor, but its effects might not be consistent for all rotor design variations, so a rigid model is appropriate here.)

Reference 8 also modeled the XV-15 rotor, but using UMARC instead of CAMRAD II. The UMARC model did not include antisymmetric airframe modes and was trimmed in windmilling (zero-power) condition.

Trim criteria

In normal flight-test operations, the aircraft is trimmed to level flight up to the power- or torque-limited airspeed, then allowed to descend as necessary to achieve the desired airspeed at the torque limit. Limited-power trim usually determines the whirl-mode stability boundary, but for some rotors, zero-power trim is the limiting condition, so both must be examined. For this research, limited-power trim always had a lower instability airspeed than zero power, although not by a large margin. Results for only the former are reported herein. Here a torque limit of 130,000 in-lb was used, reached at 275 knots with the thin wing.

The rotor was trimmed to 458 rpm (76% of hover design rpm), at sea-level standard conditions because it is a nominal design point and highlights the effects of the parametric variations. The speed range was 150 to 400 knots true airspeed, with trim and stability calculated in 25-knot increments.

Rotor design variations

Initial research efforts suggested that extending masses ahead of the blade leading edge could greatly increase whirl-mode stability (Refs. 15, 16). In classic flutter theory, the distance between the center of gravity (CG) and the aerodynamic center (AC) is a key parameter. This suggested that moving the AC aft should have similar effects to moving the CG forward. The effects of AC and CG offsets on XV-15 whirl-mode stability were therefore studied with CAMRAD II.

The rotor parametric variations were distributed among four radial segments, numbered 1 to 4 from root to tip as shown in Fig. 2. For simplicity, stepwise offsets were analyzed first. The AC was offset aft in five increments of 5% of tip chord. (Local chord was not used, lest the inboard taper confound the results by creating an effective forward sweep along part of segment #1.)

The AC shifts were effected by shifting the airfoil aft with respect to the pitch axis, which in this model is the same as the blade elastic axis (EA). The airfoil was referenced to the quarter chord (QC). Figure 2 shows an example 10% QC aft offset at the tip segment.

The CG was offset forward in increments of 5% tip chord to match the magnitudes of the QC offsets. The maximum offset was therefore 25% chord, which placed the CG at the leading edge. The two types of offset were analyzed separately. There were thus five discrete values of two parameters each, at four separate radial segments, making a matrix of 40 variations in addition to the baseline.

The stepped modifications were not intended to represent producible rotors, but to reveal the effects of the design parameters on stability. More realistic swept-tip blades were subsequently analyzed, as discussed later in this paper.

Stability Predictions

Adding up the cases discussed above, there are 11 airspeeds for both trim criteria (zero power and limited power), applied to each of the 40 parametric variations, plus the thick- and thin-wing XV-15 models with the unmodified rotor, for a total of 924 cases. It is practical to present only a general overall summary and a few specific examples.

Baseline checks

Figures 3 and 4 compare the CAMRAD II predictions for thick- and thin-wing XV-15 whirl modes, plotted as frequency and damping versus airspeed for each of the wing modes. The intersections of the individual damping curves with the zero-damping axis define the stability boundaries for each mode; the overall whirl-flutter boundary is that of the least stable mode.

There are six wing modes to be examined: beamwise bending, chordwise bending, and torsion, each in symmetric (Figs. 3(a) and 4(a)) and antisymmetric (Figs. 3(b) and 4(b)) forms. The mode labels are somewhat arbitrary because the mode shapes rarely show pure bending, torsion, or chordwise deflections. This is especially true for the antisymmetric chord and torsion modes. Moreover, the blade collective lag mode couples strongly with the wing modes at high speeds. The essential point is that all unstable modes are predicted with sufficient accuracy to reveal the effects of modifications to the rotor.

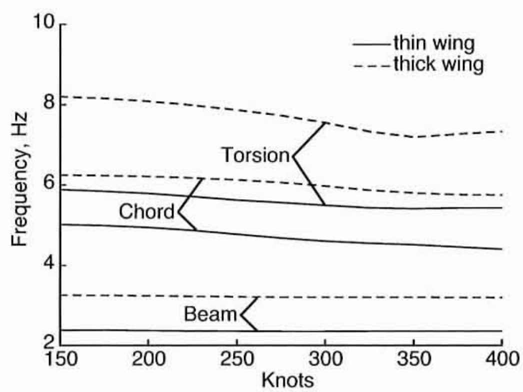

Fig. 3a. Symmetric whirl-mode frequency versus airspeed for the thick- and thin-wing models.

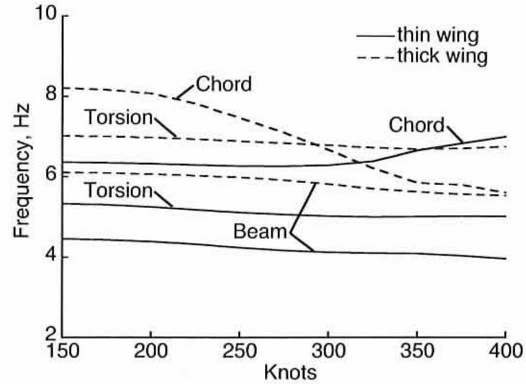

Fig. 3b. Antisymmetric whirl-mode frequency versus airspeed for the thick- and thin-wing models.

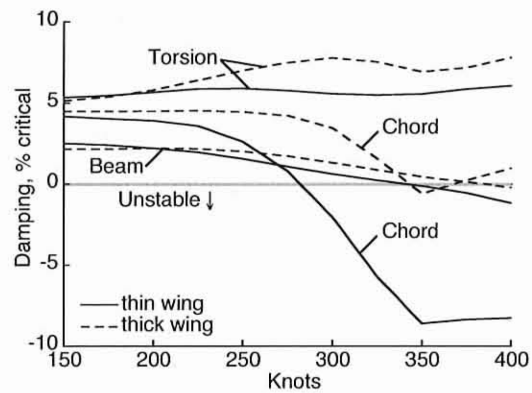

Fig. 4a. Symmetric whirl-mode damping versus airspeed for the thick- and thin-wing models.

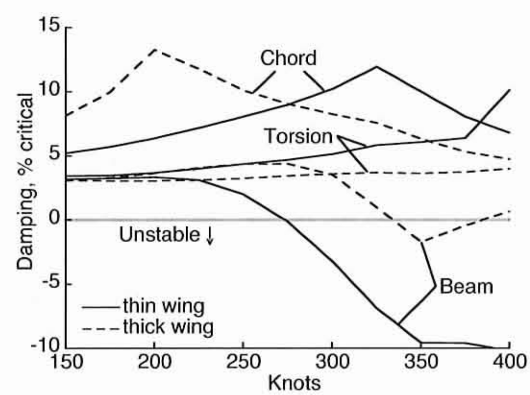

Fig. 4b. Antisymmetric whirl-mode damping versus airspeed for the thick- and thin-wing models.

Figure 4 clearly shows that symmetric chord and antisymmetric beam are the limiting modes for both the thick- and thin-wing models. It also shows that reducing the wing thickness greatly reduced the symmetric chord, antisymmetric beam, and antisymmetric chord damping. The stability boundary of the thin-wing model was barely 275 knots, a reduction of 60 knots below that of the original, thick wing. The key point is that the instability airspeed was greatly reduced without changing the basic nature of the limiting modes.

At 400 knots, the tip Mach number is 0.82, placing the tip airfoil section inside the transonic regime. The blade section lift curve slope is decreasing at that point, which improves stability. This effect can be clearly seen in Fig. 4 for symmetric chord (Fig. 4(a)) and antisymmetric beam and torsion (Fig. 4(b)).

Summary of parametric variations for stepped offsets

Figures 5 and 6 summarize the changes to the overall stability boundary caused by the variations in blade QC and CG, modeled as stepped offsets. For the analyses discussed in this section, only one type of offset was applied at a time, and at only one radial segment at a time. The thin-wing airframe model was used in all cases.

The limiting airspeed was interpolated to the nearest 5 knots for each value of offset in Figs. 5 and 6. The lower limit of each plot is 275 knots, the stability boundary for the thin-wing model with the unmodified rotor. The stability boundary of the modified rotor never dropped below this speed. The upper limit of 400 knots is the maximum speed analyzed.

Eleven of the 40 QC and CG variations increased the instability airspeed by 60 knots or more, which fully recovered the stability boundary of the original, thick-wing XV-15 model.

It is immediately apparent that QC offsets are much more effective than CG offsets: usually at least twice as much so (compare Fig. 5 to Fig. 6). Offsets at the tip are more effective than at the root for both types of offset.

The dotted lines in Fig. 6 represent the stability boundaries of the antisymmetric beam mode. Aerodynamic damping was neglected in the stability analyses. It would have increased the damping of the symmetric beam mode more than the other modes, so that all values would have shifted upwards, but by unequal amounts. The stability trends would then more closely follow the dotted bars in Fig. 6. The extended stability boundaries for segment #4 in Fig. 6 are generally similar to the boundaries of segment #2 in Fig. 5, which reveals that both types of offset have similar effects on stability, aside from the greater overall effectiveness of QC offsets.

The effects of QC offsets were more pronounced than expected. The 400-knot limit of this study prevented a complete evaluation of the ultimate effectiveness of QC offsets at very high speeds, but exploitation of large stability improvements would require a reoptimized rotor. A 400-knot-class proprotor would have different airfoils, twist and planform, and would therefore be expected to show different sensitivities to the parametric variations considered here.

The sensitivity of modal stability to the amount of QC and CG offset is revealed in more detail when the data are plotted for a single blade segment and fixed airspeed. Figures 7 and 8 present damping versus QC and CG offsets, respectively, for blade segment #4 at 350 knots. The outermost blade segment was chosen because the effects are most pronounced for that radial location. An airspeed of 350 knots was chosen because it is high enough to be strongly sensitive to both types of offset, yet not so high as to confound the results with transonic airfoil effects.

Comparing Fig. 7 to Fig. 8, any given amount of quarter-chord offset was much more effective than the same amount of center-of-gravity offset, but only for offsets less than about 10% of tip chord. Increasing the QC offset had almost no effect beyond 15%, while CG offset was effective to the limit of the analysis, although beginning to be slightly less so at 25% offset. For both types of offset, the wing modes most strongly affected were symmetric chord and antisymmetric beam. These

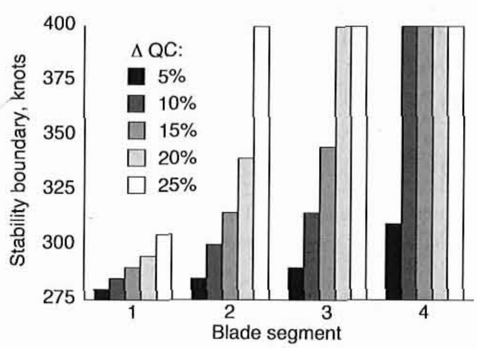

Fig. 5. Whirl-mode stability boundaries for quarter-chord offsets, thin-wing model.

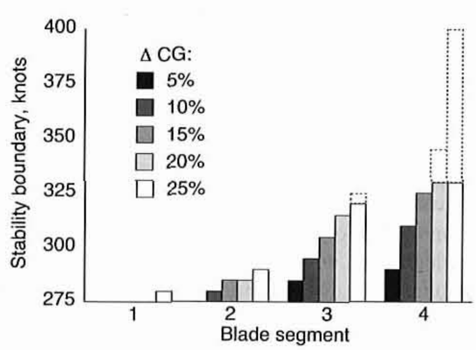

Fig. 6. Whirl-mode stability boundaries for center-of-gravity offsets, thin-wing model. Dotted bars are antisymmetric mode limits.

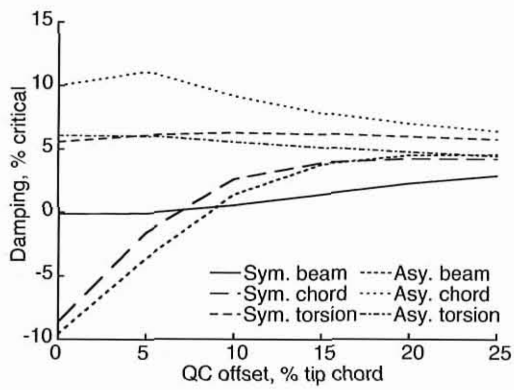

Fig. 7. Variation of damping with quarter-chord offset for blade segment #4 at 350 knots.

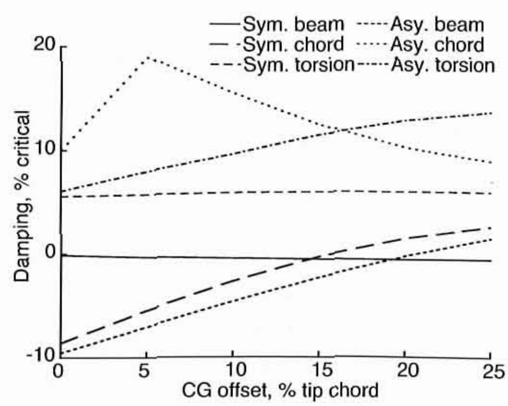

Fig. 8. Variation of damping with center-of-gravity offset for blade segment #4 at 350 knots.

are the critical modes because they are the least stable at zero offset. At a large enough value of either QC or CG offset, the damping of these two modes becomes greater than the damping of the symmetric beam mode, which is not strongly affected by either QC or CG offsets. However, this analysis included no wing aerodynamic damping, which would raise the damping of the symmetric beam mode more than any other mode.

Antisymmetric torsion was strongly influenced by CG offsets, but only slightly so by QC offsets. Antisymmetric chord was very sensitive to both offsets, and was the only mode that decreased significantly with either type of offset. Because the damping of both of these modes is already high at zero offset, the variations shown here are of little consequence.

Antisymmetric chord damping shows the peculiar behavior of a large increase for a small amount of offset, then a decrease with increasing offset; the effect is stronger for CG offsets (Fig. 8) than for QC offsets (Fig. 7). This is apparently caused by a strong interaction between wing and rotor modes, such that a small offset of either type significantly separates the modes, resulting in a large change in damping. Once the modes are separated, further changes in offset have much less effect. The reader is reminded that mode labels are somewhat arbitrary because of these and other coupling effects. The rotor modes have higher damping than the whirl modes and accordingly are not shown in the figures.

The damping curves appear to be converging to a common value of about 5% critical damping, at least for QC offsets. This is roughly the same value as for a rigid, gimbaled rotor (not shown). If the rotor did not dynamically couple with the wing at all, the wing (and nacelles) would still have a flutter boundary. A tentative conclusion is that at large enough values of QC offset, the rotor is fully stabilized and the flutter boundary is determined by the wing. Further increases to the offset would be expected to have little effect.

The speculation above is only weakly supported by Fig. 8, but CG offsets would be expected to cause different modal couplings, hence different overall levels of stability.

Combined offsets

Because of complex modal couplings plus the nonlinear sensitivity of damping to offset (Figs. 7 and 8), it cannot be assumed that QC and CG offsets will be compatible. Figures 9 and 10 illustrate combined offsets, where one type of offset is held at a fixed value while the other is varied. As in Figs. 7 and 8, offsets were applied to the outermost blade segment and stability was calculated at 350 knots. Only the least stable modes are shown.

Figure 9 shows the effects of varying QC offset while the CG offset is held at 15% chord. For comparison, damping curves for QC variations

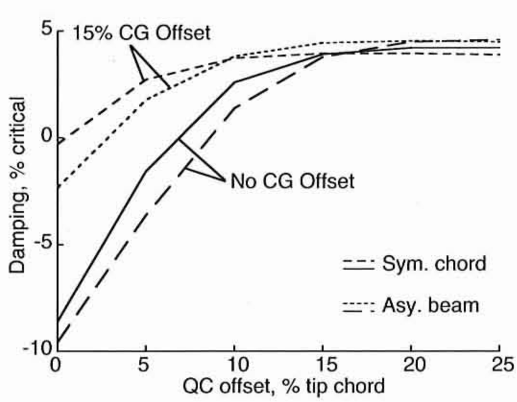

Fig. 9. Variation of damping with QC offset while CG offset is held fixed for blade segment #4 at 350 knots.

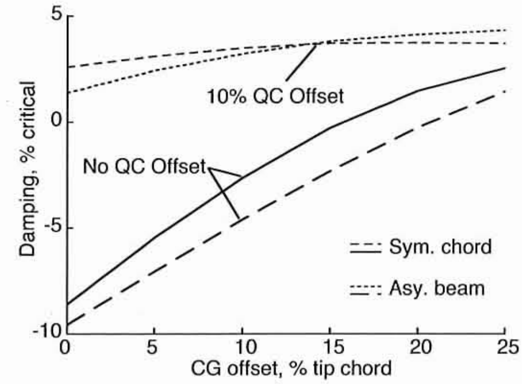

Fig. 10. Variation of damping with CG offset while QC offset is held fixed for blade segment #4 at 350 knots.

with zero CG offset are also shown. With a 15% CG offset, the damping is significantly increased for low values of QC offset, and the nonlinear sensitivity of damping to changes in offset is still evident, as is convergence to a value just under 5% damping. However, the overall sensitivity to QC offset is much reduced.

Figure 10 shows the effects of varying CG offset while the QC offset is held at 10% chord. Damping curves for CG variations with zero QC offset are also shown. Again, the damping is increased much more at low values of CG offset than at high values. The overall damping is consistently increased for combined offsets and appears to be converging towards a value slightly under 5%.

The common result is that QC and CG offsets can be combined for an increase in damping, but their effects do not add linearly. Fortunately, most of the reduction in sensitivity to offset occurs after the system is stable, so the asymptotic behavior presents no problems.

Swept-tip blades

Figures 9 and 10 together imply that swept tips would increase whirl-mode stability. Aft sweep would move the CG in an unfavorable direction, but the greater sensitivity of damping to QC offset would cause a net increase in stability. Sweep would also maximize the amount of offset at the tip for a slight improvement over a stepped offset, and would make for more practical blade construction. Note that blade sweep is derived from different considerations than apply to classic swept wings.

Figure 2 shows two blades with swept tips. The first has 5.34 deg of sweep over the outer 20% of blade radius, which gives the same offset moment as a 10%-chord offset. That is, the product of the local offset and the incremental chord, integrated over the outermost blade segment, is the same for both a 10% stepped offset and a 5.34-deg swept blade. The second swept blade has 10 deg of sweep over the outer 20% radius, the maximum analyzed in this study.

For the stability analyses discussed herein, sweep was modeled by sweeping the elastic axis (EA) and quarter-chord (QC) line, either together or separately, as explained below. In CAMRAD II, structural and aerodynamic parameters are referenced to the elastic axis and quarter-chord line, respectively, so they are automatically swept with the EA and QC (Ref. 13). Sweep was always initiated at $0.8R$ (blade segment #4 in Fig. 2); the outer 20% of the blade was, in effect, rotated aft by the amount of sweep. Damping was calculated at 2-deg increments of sweep.

Figures 11 and 12 show the variation in damping with sweep for blades with aerodynamic sweep only and with equal aerodynamic and structural sweep. The first is not a practical blade; indeed, at high values of sweep, it cannot physically exist because the center of gravity and elastic axis are both ahead of the leading edge at the tip. Nevertheless, the purely

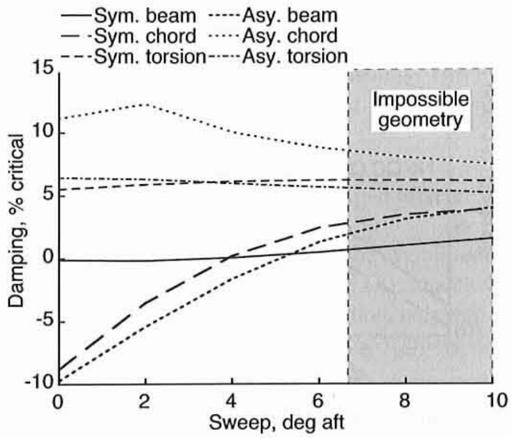

Fig. 11. Variation of damping with QC sweep at 350 knots; the structure is not swept.

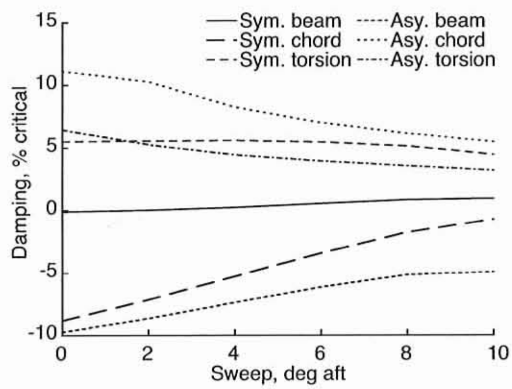

Fig. 12. Variation of damping with full sweep at 350 knots.

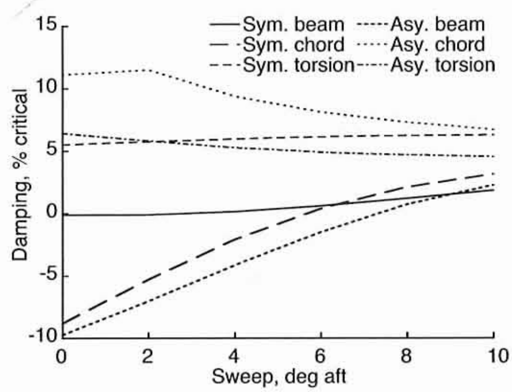

Fig. 13. Variation of damping with sweep at 350 knots; the structural sweep is one-half the aerodynamic sweep.

theoretical results are instructive because they clearly show that sweep is equivalent to a stepped offset: the damping curves in Figs. 7 and 11 are very similar.

Figure 12 shows the predicted damping for a blade with a fully swept tip. This blade is far more practical than that of Fig. 11, but the aft sweep of the CG greatly reduces the increase in damping. There is still a net improvement to stability.

Figure 13 shows results for a blade with its elastic axis and center of gravity swept one-half as much as the quarter chord. Although unconventional, such a blade would be feasible as long as the sweep did not start too far inboard. The damping of the least stable modes is much improved over that of Fig. 12; at high values of sweep, it is almost as good as that for blades with only aerodynamic sweep (Fig. 11).

It should be emphasized that all analyses reported here are based on the original XV-15 steel blades, for which the manufacturability of any modification is highly problematical. A swept tip would be more practical to implement with a modern, composite structure. Because the particular designs considered here have no likelihood of being constructed, and because the results shown in Fig. 13 are more than adequate to illustrate the benefits of the concept, no further optimization of the blade design was undertaken. A blade with 10-deg aerodynamic and 5-deg structural sweep was chosen for further study, as discussed in the following sections.

Control-system stiffness

The stiffness of the control system has a strong effect on aeroelastic stability, as shown in Fig. 14 for the baseline rotor. The baseline pitch stiffness seen by the blade is multiplied by a stiffness factor, against which damping is plotted. (The baseline value is 22,400 ft-lb/rad.) CAMRAD II allows the pitch links to be analytically locked, yielding the equivalent of infinite stiffness. Infinite stiffness yields damping values negligibly different from a stiffness factor of 100, so the stiffness scale in Fig. 14 is truncated at that value. For clarity, the scale is logarithmic to expand the damping curves at low values of stiffness while simultaneously revealing the asymptotic behavior at high values. Damping was calculated at 350 knots for the thin wing, consistent with Figs. 7–13.

Figure 14 shows that about half of the maximum increase in damping is obtained with a pitch stiffness factor of two, and further increases in stiffness yield progressively diminishing increases in damping. A stiffness factor of two was used in selected analyses below. The V-22 has roughly three times the scaled pitch stiffness of the XV-15, so a factor of two is reasonable and no further optimization was undertaken.

Figure 15 shows the results of combining tip sweep with an increased-stiffness control system. As in Fig. 13, the aerodynamic sweep was twice the structural sweep. The asymptotic behavior of damping with sweep reduces the effect of increased control stiffness (compare Fig. 15 with Fig. 13); at high enough values of sweep, the increase in damping is negligible. However, the system becomes stable at a lower value of sweep: about 5 deg instead of 7 deg, a useful improvement.

The trends of damping with airspeed are shown in Fig. 16 for combined tip sweep and increased control system stiffness. The rotor is the same as that analyzed for Fig. 15 at maximum sweep. For ease of comparison, the format is the same as Figs. 3 and 4. Note that all whirl modes, including the symmetric beam mode, show little variation in damping with airspeed; the wing/rotor system is now completely stable.

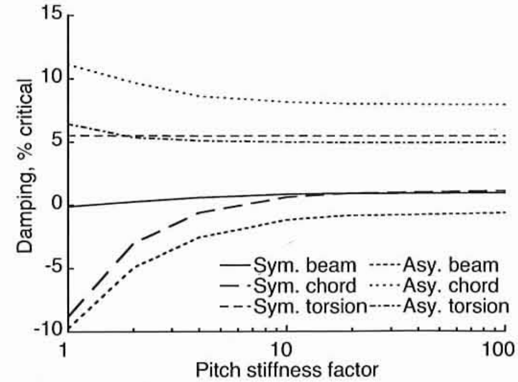

Fig. 14. Variation in damping with pitch stiffness factor for the baseline XV-15 rotor at 350 knots.

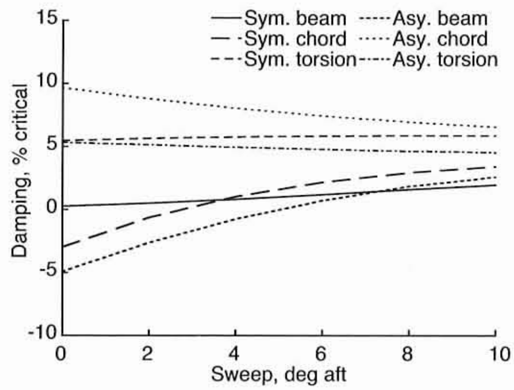

Fig. 15. Variation of damping with sweep at twice the baseline pitch stiffness at 350 knots; the structural sweep is one-half the QC sweep.

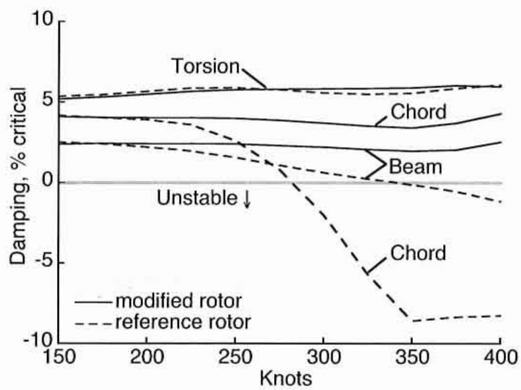

Fig. 16a. Symmetric whirl-mode damping versus airspeed at twice the baseline pitch stiffness, 10 deg QC sweep and 5 deg structural sweep.

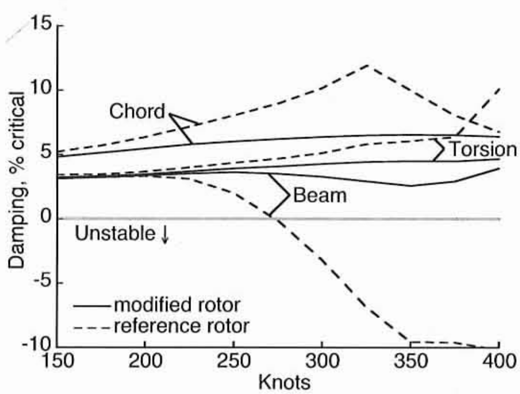

Fig. 16b. Antisymmetric whirl-mode damping versus airspeed at twice the baseline pitch stiffness, 10 deg QC sweep and 5 deg structural sweep.

Delta-three variations

So far in this paper, blade modifications have been studied for the purpose of extending the XV-15 whirl-flutter boundary for a thin wing. Improvements to whirl-mode damping can be exploited for other purposes, an example of which is discussed in the following paragraphs.

Delta-three (δ_3) is the kinematic coupling between blade flapping and pitch (Ref. 17). As defined herein, positive δ_3 causes nose-down pitching for upwards blade flapping. This *decreases* stability for some blade modes, typically lag modes. The realization that negative δ_3 is stabilizing was a major conceptual breakthrough necessary for the successful development of the XV-15 (Ref. 18).

Because the effective flapping hinge is at the center of rotation of a gimbaled rotor, a literal skewed hinge is not possible on the XV-15, so offset pitch horns must be used. Furthermore, it is extremely difficult to arrange the pitch horns to achieve small values of δ_3 without mechanical interference, especially for rotors with four or more blades. As the magnitude of δ_3 increases, whirl-mode stability rapidly decreases.

These effects constrain practical design values of δ_3 to a narrow range of negative values. The XV-15 design value of δ_3 is -15 deg (Ref. 12), realized by a trailing, offset pitch horn. All values of δ_3 discussed herein are nominal values; the actual value varies slightly as the pitch horn moves with changing collective and cyclic control inputs.

Figure 17 shows the variation of damping with δ_3 for the baseline XV-15 (thick wing) and unmodified rotor. The airspeed is 300 knots, the design maximum. The damping predicted by CAMRAD II becomes negative between -20 and -25 deg δ_3. The actual aircraft must have a margin of stability, so the design magnitude of δ_3 must be less than the zero-damping value. Figure 17 indicates that -15 deg is a reasonable value, which is consistent with XV-15 experience.

Damping of the unstable modes varies almost linearly with δ_3 until it approaches the limiting, stable value consistent with Figs. 7–15 (although maximum antisymmetric beam damping is a bit higher). Damping for positive δ_3 is not shown because certain rotor modes, principally blade lag modes coupled with wing modes, are always unstable.

Figure 18 shows results for a control-system stiffness factor of two. The value of δ_3 for zero damping is extended to almost -35 deg.

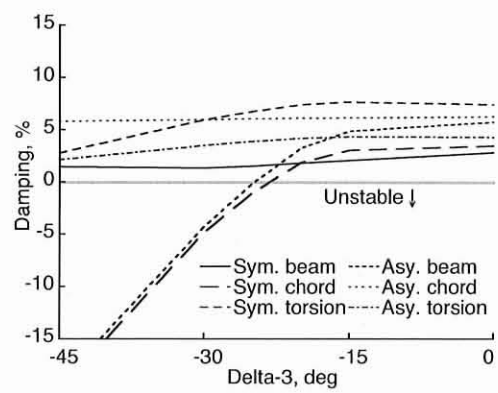

Fig. 17. Variation of damping with δ_3 for the baseline XV-15 and unmodified rotor at 300 knots.

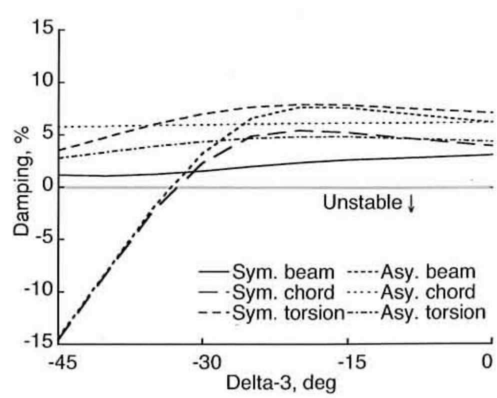

Fig. 18. Variation of damping with δ_3 for the baseline XV-15 with twice the baseline pitch stiffness at 300 knots.

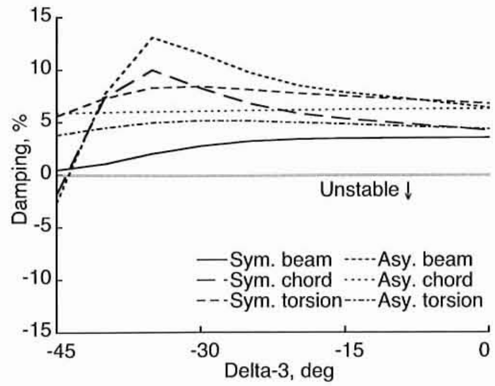

Fig. 19. Variation of damping with δ_3 for the baseline XV-15 with 10 deg QC sweep and 5 deg structural sweep at 300 knots.

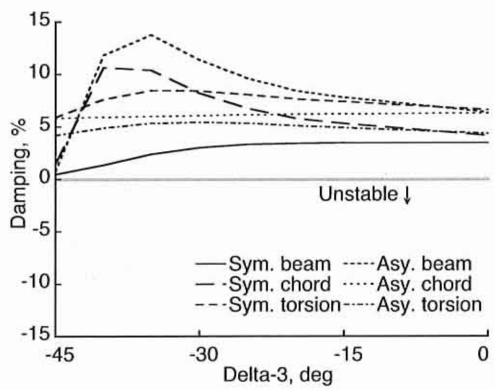

Fig. 20. Variation of damping with δ_3 for the baseline XV-15 with twice the baseline pitch stiffness, 10 deg QC sweep and 5 deg structural sweep at 300 knots.

Figure 19 shows results for a rotor with 10 deg aerodynamic sweep and 5 deg structural sweep over the outmost 20% blade radius. This is the most extreme sweep plotted in Fig. 13 and is the most effective of the practical blade designs examined here. The airspeed is 300 knots, the same as Figs. 17 and 18. The δ_3 value for neutral stability is extended to almost −45 deg. The two least stable modes at −45 deg δ_3 become the most stable modes near −35 deg, then asymptotically approach the limiting values seen in the previous plots.

The final stability analysis combined the increased control-system stiffness of Fig. 18 with the swept tip of Fig. 19; the results are shown in Fig. 20. Whirl-mode damping is positive for $\delta_3 = -45$ deg. This value of δ_3 was the maximum studied because no further increase is necessary for a four-bladed rotor, and because the incremental improvement caused by the increased control-system stiffness is very minor compared to Fig. 19.

Loads Implications

Two rotor designs were analyzed further to estimate their effects on rotor loads. Both designs used the most effective rotor developed during this study, with 10-deg aerodynamic sweep, 5-deg structural sweep, and twice the baseline control stiffness. Design A had the 15% t/c wing with −15-deg δ_3, and Design B had the 23% t/c wing with −45-deg δ_3. Two flight conditions were analyzed:

1) Airplane mode at 250 knots, 458 rpm ($\mu = 0.70$), rotor $C_T/\sigma = 0.027$.

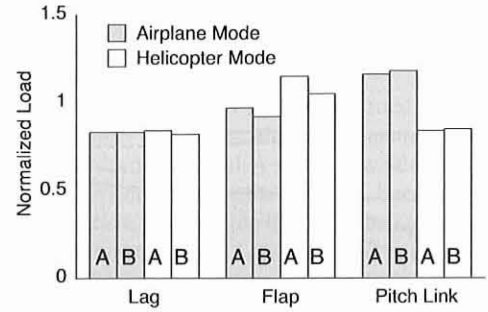

Fig. 21. Mean rotor loads, normalized to the baseline rotor, for designs A and B.

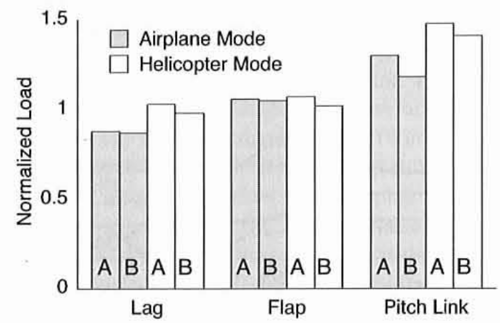

Fig. 22. Oscillatory rotor loads, normalized to the baseline rotor, for designs A and B.

2) Helicopter mode (nacelle angle = 75 deg) at 80 knots, 565 rpm ($\mu = 0.18$), rotor $C_T/\sigma = 0.088$.

The airplane mode condition was chosen to ensure that the loads were calculated within the thin-wing stability boundary (Fig. 4) to provide a valid baseline reference.

Predictions of mean and 1/2 peak-to-peak oscillatory loads are plotted in Figs. 21 and 22. The figures include flap and lag bending moments at $0.35R$ and pitch link force, all normalized to the reference (unmodified) rotor for the appropriate wing. Helicopter-mode loads are normalized to the helicopter reference, and airplane-mode loads are normalized to the airplane reference. Mean and oscillatory loads are plotted separately. The results for the example designs are plotted adjacent to each other for comparison, and airplane-mode results are plotted adjacent to helicopter-mode results for each type of load (lag, flap, and pitch-link loads). (See Ref. 15 for loads predictions for stepped-offset blades.)

All loads analyses included six harmonics of blade motion and 12 blade modes and were based on the thin-wing airframe model. In airplane mode, the analysis included wing/body interference velocities at the rotor. Uniform inflow was assumed because the differences caused by blade dynamics are of interest, for which momentum theory is adequate, especially in airplane mode. Development of a full wake model for helicopter flight was not justified at this stage of the research, which is focused on flutter, not loads. The objective of the loads analysis was to check for large adverse load variations.

Examination of Fig. 21 shows that neither of the design variations had severely adverse effects on mean loads in airplane mode. Mean flap-bending loads were almost always reduced compared to the baseline rotor.

In Fig. 22, lag- and flap-bending oscillatory loads were little affected, but pitch-link loads were significantly increased in airplane mode for both designs. However, the normalization against loads in the same flight condition exaggerates the effect. In fact, oscillatory loads were lower in airplane mode than in helicopter mode.

Although not a comprehensive loads survey, these results are enough to show that loads increases should be acceptable. No attempt was made to adjust balance weights or otherwise tune the rotor for loads, so it should be possible to reduce the loads below those shown here. The key result is that there exist combinations of parameters that give large increases in the whirl-mode stability boundary without excessive increases in loads.

Conclusions and Recommendations

The XV-15 rotor was analyzed with CAMRAD II to examine the effects on whirl-mode aeroelastic stability of chordwise offsets of the rotor blade quarter chord and center of gravity relative to the elastic axis. The XV-15 model was modified to have a thinner wing (15% t/c) to better reveal the effects of the modifications. Small rearward offsets of the quarter-chord created large increases in the stability boundary, in some cases by over 100 knots. The effect grew progressively stronger as the QC and CG offsets were shifted radially outboard. Forward offsets of the blade center of gravity had similar effects, but the maximum improvement seen was limited to 55 knots. For the range of offsets analyzed, CG offsets had a more linear effect on stability than QC offsets. Swept-tip blades showed stability improvements similar to stepped-offset designs.

Proper choice of parametric variations can avoid excessive increases in rotor loads. Limited-power trim proved slightly less stable than windmill-state trim.

These results can be applied to tiltrotors in several ways, most obviously to reduce the wing thickness for improved cruise performance while retaining adequate whirl-mode stability margins. In the present study, the wing thickness-to-chord ratio was reduced from 23% to 15% without decreasing the whirl-mode boundary. Thickness could in principle be retained while reducing weight or increasing aspect ratio, as appropriate for the performance goals of a particular design.

Offsets of the blade aerodynamic center and center of gravity, or the equivalent sweep, should be utilized as primary design variables because of their powerful effects on whirl-mode stability.

The improvements to whirl-mode stability could also be used to expand the range of delta-three (pitch-flap coupling). A sufficiently large increase in delta-three would permit designing four-bladed rotors with otherwise conventional gimbaled hubs.

The present study analyzed a broad range of large offsets. Follow-on research should examine smaller increments of the key parameters, and should focus on the outboard blade segments, where the effect is largest. This would better define optimum values and sensitivities for more realistic design values. It would also be appropriate to examine the effects for a rotor explicitly designed for very high speeds, with re-optimized twist, airfoil sections, taper, etc. The analysis could be usefully extended to more radical blade concepts, such as inverse-taper and external mass booms, and to further examine the interplay between blade design parameters and control system stiffness, delta-three, and other variables.

Acknowledgments

The authors wish to thank Franklin D. Harris for his inspiration for the research and for his constructive criticisms and enthusiastic support. The authors also wish to thank John F. Madden, whose insight led to the aerodynamic-offset analyses and whose continuing suggestions have strongly influenced the research effort.

References

[1]Maisel, M. D., Giulianetti, D. J., and Dugan, D. C., *The History of the XV-15 Tilt Rotor Research Aircraft: From Concept to Flight*, NASA SP-2000-4517, 2000.

[2]Nixon, M. W., Piatak, D. J., Corso, L. M., and Popelka, D. A., "Aeroelastic Tailoring for Stability Augmentation and Performance Enhancements of Tiltrotor Aircraft," American Helicopter Society 55th Annual Forum Proceedings, Montréal, Canada, May 25–27, 1999, Vol. 1, pp. 1013–1030.

[3]Popelka, D., Lindsay, D., Parham, T., and Berry, V., "Results of an Aeroelastic Tailoring Study for a Composite Tiltrotor Wing," American Helicopter Society 51st Annual Forum Proceedings, Fort Worth, TX, May 9–11, 1995, Vol. II, pp. 1117–1137.

[4]Nixon, M. W., "Parametric Studies for Tiltrotor Aeroelastic Stability in High Speed Flight," *Journal of the American Helicopter Society*, Vol. 38, (4), October 1993, pp. 71–79.

[5]Barkai, S., and Rand, O., "The Influence of Composite Induced Couplings on Tiltrotor Whirl-Flutter Stability," *Journal of the American Helicopter Society*, Vol. 43, (2), April 1998, pp. 133–145.

[6]van Aken, J. M., "Alleviation of Whirl-Flutter on Tilt-Rotor Aircraft Using Active Controls," American Helicopter Society 47th Annual Forum Proceedings, Phoenix, AZ, May 6–8, 1991, Vol. 2, pp. 1321–1344.

[7]Matuska, D., Sacullo, A., and Studebaker, K., "Reduced Tip Speed Testing of a Variable Diameter Tiltrotor," Nineteenth European Rotorcraft Forum, Cernobbio (Como), Italy, September 14–16, 1993.

[8]Srinivas, V., Chopra, I., and Nixon, M. W., "Aeroelastic Analysis of Advanced Geometry Tiltrotor Aircraft," *Journal of the American Helicopter Society*, Vol. 43, (3), July 1998, pp. 212–221.

[9]Detore, J. A., and Gaffey, T. M., "The Stopped-Rotor Variant of the Proprotor VTOL Aircraft," *Journal of the American Helicopter Society*, Vol. 15, (3), July 1970, pp. 45–56.

[10]Johnson, W., Lau, B. H., and Bowles, J. V., "Calculated Performance, Stability, and Maneuverability of High Speed Tilting Proprotor Aircraft," Twelfth European Rotorcraft Forum, Garmisch-Partenkirchen, Federal Republic of Germany, September 22–25, 1986.

[11]Johnson, W., "CAMRAD II Comprehensive Analytical Model of Rotorcraft Aerodynamics and Dynamics—Rotorcraft Applications," Johnson Aeronautics, Palo Alto, California, 1993.

[12]Maisel, M., "Tilt Rotor Research Aircraft Familiarization Document," NASA TN X-62, 407, January 1975.

[13]Johnson, W., "CAMRAD II Comprehensive Analytical Model of Rotorcraft Aerodynamics and Dynamics—Theory Manual," Johnson Aeronautics, Palo Alto, California, 1993.

[14]MacNeal-Schwendler Corporation, "MSC NASTRAN for Windows—Evaluation Guide and User's Manual," MSC Inc., Los Angeles, California, 1997.

[15]Acree, C. W., Peyran, R. J., and Johnson, W., "Rotor Design for Whirl Flutter: An Examination of Options for Improving Tiltrotor Aeroelastic Stability Margins," American Helicopter Society 55th Annual Forum Proceedings, Montréal, Canada, May 25–27, 1999, Vol. 1, pp. 997–1012.

[16]Madden, J. F., III, and Peyran, R. J., "Aeroelastic Stability Enhancer for Tilt-Rotor Aircraft," Invention Disclosure, NASA Case No. ARC-14298-1CU, May 1998.

[17]Johnson, W., *Helicopter Theory*, Princeton University Press, 1980.

[18]Gaffey, T. M., "The Effect of Positive Pitch-Flap Coupling (Negative δ_3) on Rotor Blade Motion Stability and Flapping," *Journal of the American Helicopter Society*, Vol. 14, (2), April 1969, pp. 49–67.